sciendo

Int. J. of Applied Mechanics and Engineering, 2022, vol.27, No.2, pp.53-76
DOI: 10.2478/ijame-2022-0019

REFLECTION AND TRANSMISSION IN NON-LOCAL COUPLE STRESS MICROPOLAR THERMOELASTIC MEDIA

DEEPA GUPTA and SANGEETA MALIK
Department of Mathematics, Baba Mastnath University, Rohtak, Haryana, INDIA
Department of Mathematics, Hindu Girls College, Sonepat, Haryana, INDIA

KRISHAN KUMAR* and RAJ KUMAR SHARMA
Department of Mathematics, Hindu College, Sonepat, Haryana, INDIA
E-mail: dahiya.krishan@gmail.com

We have studied the problem of homogenous, isotropic non-local couple stress micropolar thermoelastic solid in the absence of body forces, couple density and heat resources. The reflection and transmission of waves at the interface of two distinct media have been investigated. It is observed that amplitude ratios of various reflected and transmitted waves are functions of wave number of incident waves and are affected by the non-local parameter of thermoelastic solid.

Keywords: non-local, thermoelastic solid, amplitude ratios, reflection, transmission, couple stress, wave number.

1. Introduction

It is well known that material response to external stimuli depends on the motions of its inner structures. Classical theory ignores this effect by describing only translation degrees of freedom to material points of body. Micropolar theory of Eringen provides a model that can support body and surface couples by including intrinsic rotations of microstructure. Linear theory of micropolar elasticity was introduced by Eringen [1, 2] to deal with a class of solids which respond to micro-rotational motions and spin inertia. These types of solids can also support couple stress and distributed body couples. Eringen and Edelen [3] obtained constitutive equations through the use of localized Clausius-Duhem inequality and variational statement of Gibbsian global thermodynamics. Chandrasekharaiah [4] investigated surface waves in a homogenous isotropic linear micropolar thermoelastic half space having a stress free plane boundary and found that there exist two types of families of waves in general. One of these families is the classical thermoelastic waves which are modified under the influence of micro-elastic field and the other one is a new type of surface waves which were not encountered in classical elasticity. He obtained the explicit expressions for the displacement vector, microrotation vector, temperature and analysed the nature of deformation. Eringen [5] also developed the theory of thermo-microstretch elastic solids. These solids can stretch and contract irrespective of their translations and rotations. Inan and Eringen [6] investigated longitudinal wave propagation in thermoelastic plates in the context of nonlocal elasticity and obtained field equations using integral form of constitutive equations, balance of momenta and energy. Eringen [7] formulated theories of nonlocal elasticity, fluid dynamics and electromagnetic field that included nonlocality in both space and time. Kumar and Deswal [8] studied the variation of phase velocity with wave number for a micropolar generalized thermoelastic (MGT) and a micropolar elastic (ME) medium and observed that velocity equations are dispersive in nature. Kumar and Chawla [9] studied reflection and transmission of plane waves at an interface between elastic and micropolar diffusion media. Kumar and Gupta [10] found that the amplitude ratios of various reflected and

* To whom correspondence should be addressed

refracted waves are functions of the angle of incidence and frequency of incident waves and are influenced by the fractional order thermoelastic properties of media. Kumar et al. [11] studied reflection and transmission between two micropolar thermoelastic half-spaces with a three-phase-lag model. Kumar [12] described two types of wave propagation in a microstretch thermoelastic diffusion solid. One is "propagation of waves in a microstretch thermoelastic diffusion solid of infinite extent" and the other one is "reflection and transmission of waves at a plane interface between an inviscid fluid half space and a micropolar thermoelastic diffusion solid half space". It was observed that for a two dimensional space there exist four coupled longitudinal waves (LD, T, MD, LM) and two coupled transverse waves (CD-1 & CD-2). Kumar *et al.* [13] studied the problem of reflection due to longitudinal and transverse wave incident at a free surface of a couple stress generalised thermoelastic solid half space and found that amplitude ratios of reflected waves are influenced by the couple stress properties of the medium and also are the functions of the angle of incidence, frequency of incident wave. Khurana and Tomar [14] investigated the five basic waves consisting of three longitudinal waves and two transverse waves propagating through an isotropic non-local microstretch solid of infinite extent with distinct speeds. It was found that all waves are frequency dependent and hence dispersive in nature. Kumar [15] investigated reflection and transmission at a plane interface in a modified couple stress generalised thermoelastic solid half space and observed that amplitude ratios obtained due to incidence of a set of coupled longitudinal waves and coupled transverse waves are functions of the angle of incidence, frequency and are affected by the couple stress properties of media. Khurana and Tomar [16] investigated propagation of Rayleigh type surface waves in a nonlocal micropolar elastic solid half-space and found two modes of Rayleigh-type waves propagating under certain approximations. Singh *et al.* [17] derived governing relations and equations for a nonlocal elastic solid with voids and investigated propagation of time harmonic plane waves in an infinite nonlocal elastic solid material with voids. It was found that three basic waves consisting of two sets of coupled longitudinal waves and one independent transverse wave may travel with distinct speeds. Khurana and Tomar [18] studied reflection /transmission phenomena of plane waves at plane discontinuity separating the two distinct nonlocal micropolar solids in perfect contact. Variation of amplitude and energy ratios against the incidence angle was studied and phase shift was also depicted for incidence of a set of coupled transverse waves due to occurrence of complex valued amplitude ratios. Kaur et al. [19, 20] derived dispersion relation for the Rayleigh-type surface wave which was found to be complex in nature. It was found that only one mode of the Rayleigh-type wave exists, which faces a critical frequency same as the critical frequency of shear wave. Also, it was shown that dispersion arises due to the presence of voids and nonlocality in the medium. Sarkar and Tomar [21] investigated propagation of time harmonic plane waves in an infinite nonlocal thermoelastic solid having void pores and found there exist three sets of coupled dilatational waves and one independent transverse wave travelling with distinct speeds in the medium. All these waves were found to be dispersive in nature and influenced by a nonlocal parameter but coupled dilatational waves are attenuating while transverse waves are nonattenuating. Sarkar *et al.* [22] studied the problem of reflection of thermoelastic waves due to an incident coupled longitudinal elastic wave from the rigid and thermally insulated boundary of a homogenous, isotropic nonlocal thermoelastic half space. Singh *et al.* [23] considered the problem of reflection of plane waves from a thermally insulated surface with impedance boundary condition and also formulated appropriated potentials for incident and reflected waves satisfying boundary conditions at a plane surface. Das *et al.* [24] used GN model III and Eringen's nonlocal elasticity model to study the propagation of harmonic plane waves in a nonlocal thermoelastic medium and found two sets of coupled longitudinal waves which were dispersive in nature and experienced attenuation. In addition to the coupled waves there also exists one independent vertically shear-type wave, which is dispersive but experiences no attenuation. Biswas [25] studied the wave propagation in a nonlocal thermoelastic layer lying over a nonlocal thermoelastic half-space and derived frequency equation of Rayleigh waves. Various effects of a nonlocal parameter on the phase velocity, attenuation coefficient, specific loss and penetration depth were also discussed. Sarkar *et al.* [26] studied reflection of magneto-thermoelastic plane wave from a stress free and thermally insulated surface in a homogenous isotropic thermally conducting elastic half-space medium. Analytical expressions for the reflection coefficients and their respective energy ratios for reflected thermoelastic waves were determined. Pramanik and Biswas [27] developed a new model of non-local thermoelasticity with energy dissipation and presented graphically the phase velocity, attenuation coefficients, specific loss with respect to frequency.

Poonam and Kumar *et al.* [28] investigated the fundamental solution in a non-local couple stress micropolar thermoelastic solid with voids and observed that the non-local and void parameter had a great effect on the penetration depth, specific loss and attenuation coefficients. Kaur and Singh [29] studied the propagation of plane wave in non-local magneto-thermoelastic semiconductor solid with rotation and computed plane wave characteristics such as the phase velocity, attenuation coefficient and penetration depth of various reflected waves. Reflection and transmission problem in non-local couple stress micropolar thermoelastic media has not been studied yet. In present work, we have obtained amplitude ratios of various reflected and transmitted waves at the interface of two distinct homogenous, isotropic non-local couple stress micropolar thermoelastic solids and plotted absolute values of amplitude ratios with respect to wave number of incident P-, T-, SV1-, SV2-wave.

2. Formulation of problem

We consider a homogenous, isotropic non-local couple stress micropolar thermoelastic solid in the absence of body forces, couple density and heat sources. In three-dimensional Euclidean space E^3, let (x,y,z) be point coordinates and t represent time variable then basic equations are given by:

$$-\beta_0 \text{grad}T + (\lambda+\mu)\,\text{grad}\,\text{div}\boldsymbol{u} + (\lambda+\mu)\nabla^2\boldsymbol{u} + \kappa\text{curl}\boldsymbol{\varphi} - \rho\left(1-\varepsilon^2\nabla^2\right)\ddot{\boldsymbol{u}} = 0, \tag{2.1}$$

$$(\alpha+\beta)\,\text{grad}\,\text{div}\boldsymbol{\varphi} + \Upsilon\nabla^2\boldsymbol{\varphi} + \kappa\text{curl}\boldsymbol{u} - 2\kappa\boldsymbol{\varphi} - \rho j\left(1-\varepsilon^2\nabla^2\right)\ddot{\boldsymbol{\varphi}} = 0, \tag{2.2}$$

$$K\nabla^2 T = \left(1+\tau_0\frac{\partial}{\partial t}\right)\left(\rho C_E T' + YT_0\nabla.\dot{\boldsymbol{u}}\right) \tag{2.3}$$

where $\boldsymbol{u}$ is the displacement vector; $\boldsymbol{\varphi}=(0,\varphi,0)$ is the rotational vector; β_0 is the coefficient of linear thermal expansion; T is the temperature change measured from the absolute temperature T_0; λ and μ are Lame's constants; α,β,Υ and κ are micropolar constants; ρ is the density of the medium; ∇^2 denotes the Laplacian operator; $\varepsilon=e_0a'$ is the non-local parameter; e_0 corresponds to the material constant; a' denotes the characteristic length; j is micro-inertia; τ_0 denotes relaxation time; K is the thermal conductivity; C_E is the specific heat, $Y=(3\lambda+2\mu)\beta_0$ and dot signifies the differentiation with respect to time.

For a two-dimensional problem, we suppose that all quantities related to the medium are functions of Cartesian coordinates x,z and time t and are independent of $y\left(i.e.\frac{\partial}{\partial y}\equiv 0\right)$. We take displacement vector as:

$$\boldsymbol{u}=(u_1,0,u_3). \tag{2.4}$$

The displacement vector $\boldsymbol{u}$ is related to the potential functions $\psi_1(x,z,t)$ and $\psi_2(x,z,t)$ as:

$$u_1=\frac{\partial\psi_1}{\partial x}+\frac{\partial\psi_2}{\partial z}, \qquad u_3=\frac{\partial\psi_1}{\partial z}-\frac{\partial\psi_2}{\partial x}. \tag{2.5}$$

Basic Eqs. (2.1)-(2.2) are obtained by using governing equations:

$$\sigma_{ij,j}=\rho\ddot{u}_i, \tag{2.6}$$

$$e_{ijk}\sigma_{jk} + \mu_{ji,j} = \rho j\ddot{\varphi}_i \tag{2.7}$$

and constitutive equations

$$\left(1-\varepsilon^2\nabla^2\right)\sigma_{ij} = \lambda\delta_{ij}u_{k,k} + \mu u_{j,i} + (\mu+\kappa)u_{i,j} + \kappa e_{ijk}\varphi_k - \beta_0 T\delta_{ij}\,, \tag{2.8}$$

$$\left(1-\varepsilon^2\nabla^2\right)\mu_{ij} = \alpha\delta_{ij}\varphi_{k,k} + \beta\varphi_{j,i} + \Upsilon\varphi_{i,j}\,, \tag{2.9}$$

in a homogenous isotropic non local couple stress micropolar thermoelastic solid in the absence of body force, couple density and heat sources, where σ_{ij} are the stress components; μ_{ij} are the components of couple stress; δ_{ij} is the Kronecker delta; e_{ijk} is the permutation symbol and the comma symbol denotes spatial derivatives. For simplification, we introduce the following dimensionless quantities:

$$\begin{gathered} x' = c_0\eta_0 x, \qquad z' = c_0\eta_0 z, \qquad u_1' = c_0\eta_0 u_1, \qquad u_3' = c_0\eta_0 u_3\,, \quad t' = c_0^2\eta_0 t, \\ T' = \frac{T}{T_0}, \quad \varphi' = \frac{\kappa}{\kappa+\mu}\varphi, \quad \sigma_{ij}' = \frac{\sigma_{ij}}{\kappa+\mu}, \quad \mu_{ij}' = \frac{\kappa}{c_0\eta_0(\kappa+\mu)\Upsilon}\mu_{ij} \end{gathered} \tag{2.10}$$

where $c_0^2 = \dfrac{\lambda+2\mu}{\rho}$, $\qquad \eta_0 = \dfrac{\rho C_E}{K}$.

Now using Eq. (2.10) in Eqs (2.1)-(2.3); the field equations take the form:

$$\beta_3\frac{\partial T}{\partial x} + \beta_1^2\frac{\partial^2 u_1}{\partial x^2} + \left(\beta_1^2-1\right)\frac{\partial^2 u_3}{\partial x\partial z} + \frac{\partial^2 u_1}{\partial z^2} - \frac{\partial\varphi}{\partial z} - \beta_2^2\ddot{u}_1 + \beta_4^2\nabla^2\ddot{u}_1 = 0\,, \tag{2.11}$$

$$\beta_3\frac{\partial T}{\partial z} + \left(\beta_1^2-1\right)\frac{\partial^2 u_1}{\partial x\partial z} + \beta_1^2\frac{\partial^2 u_3}{\partial z^2} + \frac{\partial^2 u_3}{\partial x^2} + \frac{\partial\varphi}{\partial x} - \beta_2^2\ddot{u}_3 + \beta_4^2\nabla^2\ddot{u}_3 = 0\,, \tag{2.12}$$

$$\frac{\partial^2\varphi}{\partial x^2} + \frac{\partial^2\varphi}{\partial z^2} - g_1\left(\frac{\partial u_3}{\partial x} - \frac{\partial u_1}{\partial z}\right) - g_2\varphi - g_3\ddot{\varphi} + g_4\nabla^2\ddot{\varphi} = 0\,, \tag{2.13}$$

$$\frac{\partial^2 T}{\partial x^2} + \frac{\partial^2 T}{\partial z^2} = \left(\frac{\partial}{\partial t} + h_1\frac{\partial^2}{\partial t^2}\right)\left[T + h_2\left(\frac{\partial u_1}{\partial x} + \frac{\partial u_3}{\partial z}\right)\right], \tag{2.14}$$

where

$$\beta_1^2 = \frac{\lambda+2\mu+\kappa}{\kappa+\mu}, \qquad \beta_2^2 = \frac{\rho c_0^2}{\kappa+\mu}\,, \qquad \beta_3 = \frac{\beta_0 T_0}{\kappa+\mu}, \qquad \beta_4^2 = \rho\varepsilon^2 c_0^4\eta_0^2,$$

$$g_1 = \frac{\kappa^2}{(\kappa+\mu)c_0^2\eta_0^2\Upsilon}\,, \qquad g_2 = \frac{2\kappa}{c_0^2\eta_0^2\Upsilon}\,, \qquad g_3 = \frac{\rho j c_0^2}{\Upsilon}, \qquad g_4 = \frac{\rho j\varepsilon^2 c_0^4\eta_0^2}{\Upsilon},$$

$$h_1 = \tau_0 \eta_0 c_0^2 \ , \quad h_2 = \frac{\Upsilon}{\kappa \eta_0}$$

and the constitutive equations (2.8), (2.9) take the form:

$$\left(1 - \delta_1 \nabla^2\right) \sigma_{zz} = \beta_1^2 \frac{\partial u_3}{\partial z} + \delta_2 \frac{\partial u_1}{\partial x} + \beta_3 T \,, \tag{2.15}$$

$$\left(1 - \delta_1 \nabla^2\right) \sigma_{zx} = \delta_3 \frac{\partial u_1}{\partial z} + \frac{\partial u_3}{\partial x} + \varphi, \tag{2.16}$$

$$\left(1 - \delta_1 \nabla^2\right) \mu_{zy} = \frac{\partial \varphi}{\partial z} \tag{2.17}$$

where $\delta_1 = \varepsilon^2 c_0^2 \eta_0^2$, $\delta_2 = \dfrac{\lambda}{\kappa + \mu}$, $\delta_3 = \dfrac{\mu}{\kappa + \mu}$.

Using Eq.(2.5) in (2.11)-(2.14), we obtain:

$$\begin{aligned} &\beta_3 \frac{\partial T}{\partial x} + \beta_1^2 \nabla^2 \frac{\partial \psi_1}{\partial x} + \nabla^2 \frac{\partial \psi_2}{\partial z} - \frac{\partial \varphi}{\partial z} - \beta_2^2 \frac{\partial^2}{\partial t^2}\left(\frac{\partial \psi_1}{\partial x} + \frac{\partial \psi_2}{\partial z}\right) + \\ &+ \beta_4^2 \nabla^2 \frac{\partial^2}{\partial t^2}\left(\frac{\partial \psi_1}{\partial x} + \frac{\partial \psi_2}{\partial z}\right) = 0, \end{aligned} \tag{2.18}$$

$$\begin{aligned} &\beta_3 \frac{\partial T}{\partial z} + \beta_1^2 \nabla^2 \frac{\partial \psi_1}{\partial z} - \nabla^2 \frac{\partial \psi_2}{\partial x} - \frac{\partial \varphi}{\partial x} - \beta_2^2 \frac{\partial^2}{\partial t^2}\left(\frac{\partial \psi_1}{\partial z} - \frac{\partial \psi_2}{\partial x}\right) + \\ &+ \beta_4^2 \nabla^2 \frac{\partial^2}{\partial t^2}\left(\frac{\partial \psi_1}{\partial z} - \frac{\partial \psi_2}{\partial x}\right) = 0, \end{aligned} \tag{2.19}$$

$$\left(\nabla^2 - g_2 - g_3 \frac{\partial^2}{\partial t^2} + g_4 \nabla^2 \frac{\partial^2}{\partial t^2}\right) \varphi = -g_1 \nabla^2 \psi_2, \tag{2.20}$$

$$\nabla^2 T = \left(\frac{\partial}{\partial t} + h_1 \frac{\partial^2}{\partial t^2}\right)\left(T + h_2 \nabla^2 \psi_1\right). \tag{2.21}$$

Without loss of generality, we assume that all quantities are initially zero. Then Eqs (2.18) and (2.19) reduce to the following form:

$$\left(\nabla^2 - \beta_5 \frac{\partial^2}{\partial t^2} + \beta_6 \nabla^2 \frac{\partial^2}{\partial t^2}\right) \psi_1 = \beta_7 T, \tag{2.22}$$

$$\left(-\nabla^2 + \beta_2^2 \frac{\partial^2}{\partial t^2} + \beta_4^2 \nabla^2 \frac{\partial^2}{\partial t^2}\right) \psi_2 = -\varphi, \tag{2.23}$$

where $\beta_5 = \frac{\beta_2^2}{\beta_1^2}$, $\beta_6 = \frac{\beta_4^2}{\beta_1^2}$, $\beta_7 = \frac{-\beta_3}{\beta_1^2}$.

3. Plane wave analysis

$$\left\{\psi_1, \psi_2, T, \varphi, \sigma_{ij}, \mu_{ij}\right\} = \left\{\psi_1^*, \psi_2^*, T^*, \varphi^*, \sigma_{ij}^*, \mu_{ij}^*\right\}(z)\exp(wt + iax) \tag{3.1}$$

where w is the angular frequency and a is the wave number.

Using Eq. (3.1) in Eqs (2.20)-(2.23), we obtain:

$$\left(D^2 - \varepsilon_2\right)T^* = \varepsilon_3\left(D^2 - a^2\right)\psi_1^*, \tag{3.2}$$

$$\left(D^2 - \varepsilon_4\right)\varphi^* = \varepsilon_5\left(D^2 - a^2\right)\psi_2^*, \tag{3.3}$$

$$\left(D^2 - \varepsilon_6\right)\psi_1^* = \varepsilon_7 T^*, \tag{3.4}$$

$$\left(D^2 - \varepsilon_8\right)\psi_2^* = \varepsilon_9 \varphi^* \tag{3.5}$$

where

$$\varepsilon_1 = 1 + h_1 w, \quad \varepsilon_2 = a^2 + \varepsilon_1, \quad \varepsilon_3 = \varepsilon_1 h_2,$$

$$\varepsilon_4 = \frac{a^2 + g_2 + g_3 w^2 + g_4 w^2 a^2}{1 + g_4 w^2}, \quad \varepsilon_5 = \frac{-g_1}{1 + g_4 w^2}, \quad \varepsilon_6 = a^2 + \frac{\beta_5 w^2}{1 + \beta_6 w^2},$$

$$\varepsilon_7 = \frac{\beta_7}{1 + \beta_6 w^2}, \quad \varepsilon_8 = a^2 + \frac{\beta_2^2 w^2}{1 + \beta_4^2 w^2}, \quad \varepsilon_9 = \frac{1}{1 + \beta_4^2 w^2}.$$

Solving Eqs (3.2), (3.4) for T^*, ψ_1^* and Eqs (3.3), (3.5)for φ^*, ψ_2^* ,we get:

$$\left(D^4 - A_1 D^2 + B_1\right)\left(\psi_1^*, T^*\right) = 0, \tag{3.6}$$

$$\left(D^4 - A_2 D^2 + B_2\right)\left(\psi_2^*, \varphi^*\right) = 0 \tag{3.7}$$

where

$$A_1 = \varepsilon_6 + \varepsilon_2 + \varepsilon_3\varepsilon_7, \quad B_1 = \varepsilon_2\varepsilon_6 + \varepsilon_3\varepsilon_7 a^2,$$

$$A_2 = \varepsilon_4 + \varepsilon_8 + \varepsilon_9\varepsilon_5, \quad B_2 = \varepsilon_4\varepsilon_8 + \varepsilon_9\varepsilon_5 a^2.$$

Solutions of Eqs (3.6), (3.7) are given as follows:

$$\psi_1^*(z) = \sum_{j=1}^{2} L_j(a,w) e^{-\lambda_j z} + \sum_{j=3}^{4} L_j(a,w) e^{\lambda_j z}, \tag{3.8}$$

$$T^*(z) = \sum_{j=1}^{2} L_j'(a,w) e^{-\lambda_j z} + \sum_{j=3}^{4} L_j'(a,w) e^{\lambda_j z}, \tag{3.9}$$

$$\psi_2^*(z) = \sum_{j=5}^{6} L_j(a,w) e^{-\lambda_j z} + \sum_{j=7}^{8} L_j(a,w) e^{\lambda_j z}, \tag{3.10}$$

$$\varphi^*(z) = \sum_{j=5}^{6} L_j'(a,w) e^{-\lambda_j z} + \sum_{j=7}^{8} L_j'(a,w) e^{\lambda_j z}. \tag{3.11}$$

where $L_j(a,w)$ and $L_j'(a,w)$ $(j = 1,2.....8)$ are parameters depending on a and w and $\lambda_j\,(j = 1,2,3,4)$ are roots of equation: $\lambda^4 - A_1\lambda^2 + B_1 = 0$, whereas $\lambda_j\,(j = 5,6,7,8)$ are roots of equation: $\lambda^4 - A_2\lambda^2 + B_2 = 0$
Using Eqs (3.8), (3.9) in Eq. (3.4) and Eqs (3.10), (3.11) in Eq. (3.5), we obtain:

$$L_j'(a,w) = \left(\frac{\lambda_j^2 - \varepsilon_6}{\varepsilon_7}\right) L_j(a,w), \qquad (j = 1,2,3,4), \tag{3.12}$$

$$L_j'(a,w) = \left(\frac{\lambda_j^2 - \varepsilon_8}{\varepsilon_9}\right) L_j(a,w), \qquad (j = 5,6,7,8). \tag{3.13}$$

Using Eqs (35), (36) in Eqs (32), (34) we obtain:

$$T^*(z) = \sum_{j=1}^{2}\left(\frac{\lambda_j^2 - \varepsilon_6}{\varepsilon_7}\right) L_j(a,w) e^{-\lambda_j z} + \sum_{j=3}^{4}\left(\frac{\lambda_j^2 - \varepsilon_6}{\varepsilon_7}\right) L_j(a,w) e^{\lambda_j z}, \tag{3.14}$$

$$\varphi^*(z) = \sum_{j=5}^{6}\left(\frac{\lambda_j^2 - \varepsilon_8}{\varepsilon_9}\right) L_j(a,w) e^{-\lambda_j z} + \sum_{j=7}^{8}\left(\frac{\lambda_j^2 - \varepsilon_8}{\varepsilon_9}\right) L_j(a,w) e^{\lambda_j z}. \tag{3.15}$$

Using Eqs (2.5), (3.1), (3.8) and (3.10), we obtain the displacement components as:

$$u_1^* = (ia)\sum_{j=1}^{2} L_j e^{-\lambda_j z} + (ia)\sum_{j=3}^{4} L_j e^{\lambda_j z} - \sum_{j=5}^{6}\lambda_j L_j e^{-\lambda_j z} + \sum_{j=7}^{8}\lambda_j L_j e^{\lambda_j z}, \tag{3.16}$$

$$u_3^* = -\sum_{j=1}^{2}\lambda_j L_j e^{-\lambda_j z} + \sum_{j=3}^{4}\lambda_j L_j e^{\lambda_j z} - (ia)\sum_{j=5}^{6} L_j e^{-\lambda_j z} - (ia)\sum_{j=7}^{8} L_j e^{\lambda_j z}. \tag{3.17}$$

To obtain the stress and couple components, using Eqs (2.15), (2.16), (2.17), (3.1) and Eqs (3.14)-(3.17), we obtain the following:

$$t_{zz}^{*}=\sum_{j=1}^{2}\alpha_{1j}L_{j}e^{-\lambda_{j}z}+\sum_{j=3}^{4}\alpha_{1j}L_{j}e^{\lambda_{j}z}+\sum_{j=5}^{6}\beta_{1j}L_{j}e^{-\lambda_{j}z}-\sum_{j=7}^{8}\beta_{1j}L_{j}e^{\lambda_{j}z}, \tag{3.18}$$

$$t_{zx}^{*}=\sum_{j=1}^{2}\alpha_{2j}L_{j}e^{-\lambda_{j}z}-\sum_{j=3}^{4}\alpha_{2j}L_{j}e^{\lambda_{j}z}+\sum_{j=5}^{6}\beta_{2j}L_{j}e^{-\lambda_{j}z}+\sum_{j=7}^{8}\beta_{2j}L_{j}e^{\lambda_{j}z}, \tag{3.19}$$

$$m_{zy}^{*}=\sum_{j=5}^{6}\alpha_{3j}L_{j}e^{-\lambda_{j}z}-\sum_{j=7}^{8}\alpha_{3j}L_{j}e^{\lambda_{j}z} \tag{3.20}$$

where

$$\begin{aligned}&\left(1-\delta_{1}\left(D^{2}-a^{2}\right)\right)\sigma_{zz}^{*}=t_{zz}^{*},\\ &\left(1-\delta_{1}\left(D^{2}-a^{2}\right)\right)\sigma_{zx}^{*}=t_{zx}^{*},\\ &\left(1-\delta_{1}\left(D^{2}-a^{2}\right)\right)\mu_{zy}^{*}=m_{zy}^{*}\end{aligned} \tag{3.21}$$

and

$$\alpha_{ij}=-\delta_{2}a^{2}+\beta_{1}^{2}\lambda_{j}^{2}+\beta_{3}\left(\frac{\lambda_{j}^{2}-\varepsilon_{6}}{\varepsilon_{7}}\right),\quad \alpha_{2j}=-\delta_{1}(ia)\lambda_{j}-(ia)\lambda_{j},\quad \alpha_{3j}=-\lambda_{j}\left(\frac{\lambda_{j}^{2}-\varepsilon_{8}}{\varepsilon_{9}}\right),$$

$$\beta_{1j}=-\delta_{2}(ia)\lambda_{j}+\beta_{1}^{2}(ia)\lambda_{j},\quad \beta_{2j}=\delta_{1}\lambda_{j}^{2}+a^{2}+\left(\frac{\lambda_{j}^{2}-\varepsilon_{8}}{\varepsilon_{9}}\right).$$

4. Reflection and transmission

We consider longitudinal waves (P), thermal waves (T), transverse waves (SV1 and SV2) propagating through medium M and incident on the plane $z=0$. Corresponding to every incident wave, we obtain reflected longitudinal wave (P), thermal wave (T), transverse waves (SV1 and SV2) in medium M and transmitted longitudinal wave (P), thermal wave (T), transverse waves (SV1 and SV2) in medium $\bar{M}$ as shown in Fig.1.

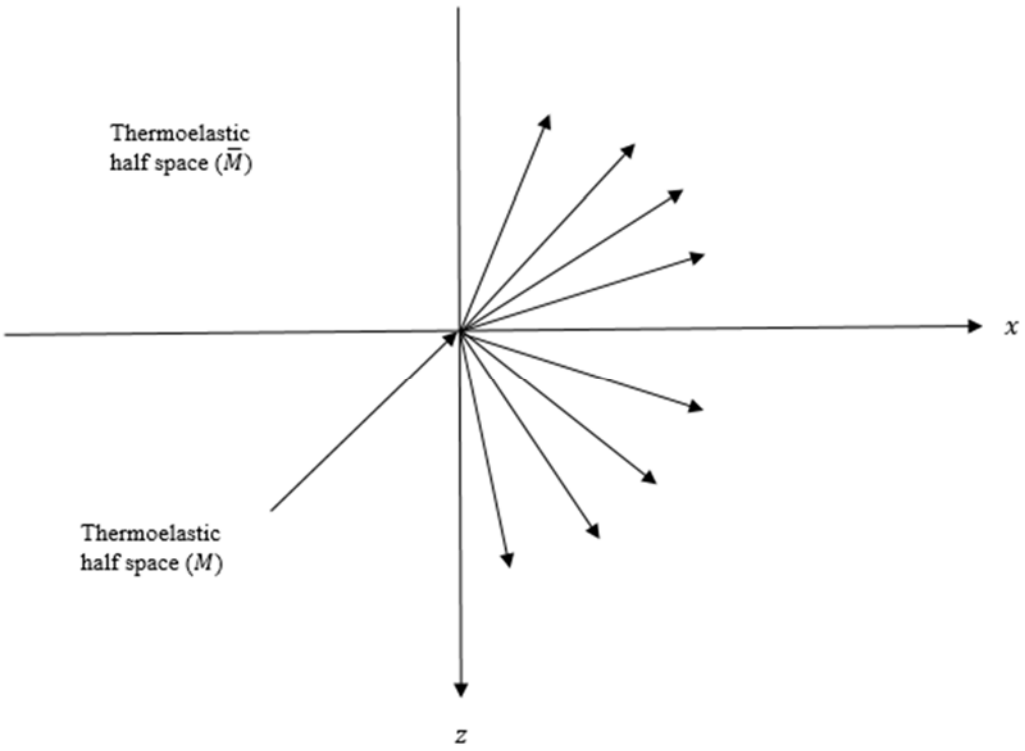

Fig.1. Geometry of the problem.

5. Application

Consider two distinct homogenous, isotropic non-local couple stress micropolar thermoelastic semi-infinite spaces separated by a plane interface $z=0$ (xy plane), the z-axis is taken normal to the xy plane vertically downward. We denote medium $M=\{(x,y,z):-\infty<x,y<\infty,\ 0\le z<\infty\}$ as the lower half space and medium $\overline{M}=\{(x,y,z):-\infty<x,y<\infty,\ -\infty<z\le 0\}$ as the upper half space. All quantities in medium $\overline{M}$ are denoted with bar and in medium M without bar. The appropriate boundary conditions are the continuity of stress components, couple components, displacement and microrotation at the interface of two half spaces. In view of the above boundary conditions, it can be written as:

$$\left(1-\overline{\delta_1}\left(D^2-\overline{a^2}\right)\right)\overline{\sigma^*_{zz}}=\left(1-\delta_1\left(D^2-a^2\right)\right)\sigma^*_{zz},$$

$$\left(1-\overline{\delta_1}\left(D^2-\overline{a^2}\right)\right)\overline{\sigma^*_{zx}}=\left(1-\delta_1\left(D^2-a^2\right)\right)\sigma^*_{zx},$$

$$\left(1-\overline{\delta_1}\left(D^2-\overline{a^2}\right)\right)\overline{\mu^*_{zy}}=\left(1-\delta_1\left(D^2-a^2\right)\right)\mu^*_{zy},$$

$$\overline{u_1^*}=u_1^*,\quad \overline{u_3^*}=u_3^*,\quad \overline{T^*}=T^*,\quad \overline{\varphi^*}=\varphi^*,\quad \overline{K}\frac{\partial\overline{T^*}}{\partial z}=K\frac{\partial T^*}{\partial z}\quad \text{at}\quad z=0.$$

Now using Eqs (44), boundary conditions may be expressed as:

$$\overline{t_{zz}^*} = t_{zz}^*\ ,\quad \overline{t_{zx}^*} = t_{zx}^*\ ,\quad \overline{m_{zy}^*} = m_{zy}^*\ ,\quad \overline{u_1^*} = u_1^*,\quad \overline{u_3^*} = u_3^*,\quad \overline{\varphi^*} = \varphi^*,$$

$$\overline{T^*} = T^*,\quad \bar{K}\frac{\partial \overline{T^*}}{\partial z} = K\frac{\partial T^*}{\partial z} \quad \text{at} \quad z = 0. \tag{5.1}$$

For medium M the values of $u_1^*, u_3^*, T^*, \varphi^*, t_{zz}^*, t_{zx}^*, m_{zy}^*$ are given by (3.14)-(3.20) and for medium $\bar{M}$ are given by:

$$\overline{u_1^*} = (i\bar{a})\sum_{j=1}^{2}\overline{L_j}e^{\overline{\lambda_j}z} + \sum_{j=3}^{4}\overline{\lambda_j}\,\overline{L_j}e^{\overline{\lambda_j}z}, \tag{5.2}$$

$$\overline{u_3^*} = \sum_{j=1}^{2}\overline{\lambda_j}\,\overline{L_j}e^{\overline{\lambda_j}z} - (i\bar{a})\sum_{j=3}^{4}\overline{L_j}e^{\overline{\lambda_j}z}, \tag{5.3}$$

$$\overline{T^*} = \sum_{j=1}^{2}\left(\frac{\overline{\lambda_j}^2 - \overline{\varepsilon_6}}{\overline{\varepsilon_7}}\right)\overline{L_j}e^{\overline{\lambda_j}z}, \tag{5.4}$$

$$\overline{\varphi^*} = \sum_{j=3}^{4}\left(\frac{\overline{\lambda_j}^2 - \overline{\varepsilon_8}}{\overline{\varepsilon_9}}\right)\overline{L_j}e^{\overline{\lambda_j}z}, \tag{5.5}$$

$$\overline{t_{zz}^*} = \sum_{j=1}^{2}\overline{\alpha_{1j}}\,\overline{L_j}\,e^{\overline{\lambda_j}z} - \sum_{j=3}^{4}\overline{\beta_{1j}}\,\overline{L_j}e^{\overline{\lambda_j}z}, \tag{5.6}$$

$$\overline{t_{zx}^*} = -\sum_{j=1}^{2}\overline{\alpha_{2j}}\,\overline{L_j}\,e^{\overline{\lambda_j}z} + \sum_{j=3}^{4}\overline{\beta_{2j}}\,\overline{L_j}e^{\overline{\lambda_j}z}, \tag{5.7}$$

$$\overline{m_{zy}^*} = -\sum_{j=3}^{4}\overline{\alpha_{3j}}\,\overline{L_j}\,e^{\overline{\lambda_j}z}. \tag{5.8}$$

Making use of boundary conditions given by (5.1) with the aid of (3.14)-(3.20) and (5.2)-(5.8), we get a system of eight non-homogenous equations which can be written as:

$$\sum_{j=1}^{8}C_{ij}y_j = d_i \qquad i = 1,2,3\ldots\ldots 8 \tag{5.9}$$

where

$$C_{11} = ia,\quad C_{12} = ia,\quad C_{13} = \lambda_7,\quad C_{14} = \lambda_8,\quad C_{15} = -i\bar{a},\quad C_{16} = -i\bar{a},\quad C_{17} = -\overline{\lambda_7},$$

$$C_{18}=-\overline{\lambda_8},\quad C_{21}=\lambda_3,\quad C_{22}=\lambda_4,\quad C_{23}=-ia,\quad C_{24}=-ia,\quad C_{25}=-\overline{\lambda_1},\quad C_{26}=-\overline{\lambda_2},$$

$$C_{27}=i\overline{a},\quad C_{28}=i\overline{a},\quad C_{31}=\alpha_{13},\quad C_{32}=\alpha_{14},\quad C_{33}=-\beta_{17},\quad C_{34}=-\beta_{18},\quad C_{35}=-\overline{\alpha_{11}},$$

$$C_{36}=-\overline{\alpha_{12}},\quad C_{37}=\overline{\beta_{13}},\quad C_{38}=\overline{\beta_{14}},\quad C_{41}=-\alpha_{23},\quad C_{42}=-\alpha_{24},\quad C_{43}=\beta_{27},\quad C_{44}=\beta_{28},$$

$$C_{45}=\overline{\alpha_{21}},\quad C_{46}=\overline{\alpha_{22}},\quad C_{47}=-\overline{\beta_{23}},\quad C_{48}=-\overline{\beta_{24}},\quad C_{51}=0,\quad C_{52}=0,\quad C_{53}=-\alpha_{37},$$

$$C_{54}=-\alpha_{38},\quad C_{55}=0,\quad C_{56}=0,\quad C_{57}=\overline{\alpha_{33}},\quad C_{58}=\overline{\alpha_{34}},\quad C_{61}=0,\quad C_{62}=0,$$

$$C_{63}=\frac{\lambda_7^2-\varepsilon_8}{\varepsilon_9},\quad C_{64}=\frac{\lambda_8^2-\varepsilon_8}{\varepsilon_9},\quad C_{65}=0,\quad C_{66}=0,\quad C_{67}=-\frac{\overline{\lambda_3}^2-\overline{\varepsilon_8}}{\overline{\varepsilon_9}},\quad C_{68}=-\frac{\overline{\lambda_4}^2-\overline{\varepsilon_8}}{\overline{\varepsilon_9}},$$

$$C_{71}=\frac{\lambda_3^2-\varepsilon_6}{\varepsilon_7},\quad C_{72}=\frac{\lambda_4^2-\varepsilon_6}{\varepsilon_7},\quad C_{73}=0,\quad C_{74}=0,\quad C_{75}=-\frac{\overline{\lambda_1}^2-\overline{\varepsilon_6}}{\overline{\varepsilon_7}},\quad C_{76}=-\frac{\overline{\lambda_2}^2-\overline{\varepsilon_6}}{\overline{\varepsilon_7}},$$

$$C_{77}=0,\quad C_{78}=0,\quad C_{81}=K\lambda_3\left(\frac{\lambda_3^2-\varepsilon_6}{\varepsilon_7}\right),\quad C_{82}=K\lambda_4\left(\frac{\lambda_4^2-\varepsilon_6}{\varepsilon_7}\right),\quad C_{83}=0,\quad C_{84}=0,$$

$$C_{85}=-\overline{K}\overline{\lambda_1}\left(\frac{\overline{\lambda_1}^2-\overline{\varepsilon_6}}{\overline{\varepsilon_7}}\right),\quad C_{86}=-\overline{K}\overline{\lambda_2}\left(\frac{\overline{\lambda_2}^2-\overline{\varepsilon_6}}{\overline{\varepsilon_7}}\right),\quad C_{87}=0,\quad C_{88}=0,$$

$$y_1=\frac{L_3}{L},\quad y_2=\frac{L_4}{L},\quad y_3=\frac{L_7}{L},\quad y_4=\frac{L_8}{L},\quad y_5=\frac{\overline{L_1}}{L},\quad y_6=\frac{\overline{L_2}}{L},\quad y_7=\frac{\overline{L_3}}{L},\quad y_8=\frac{\overline{L_4}}{L}.$$

For incident P-wave:

$$L=L_1,\quad L_2=L_5=L_6=0,$$

$$d_1=-ia,\ d_2=\lambda_1,\ d_3=-\alpha_{11},\ d_4=-\alpha_{21},\ d_5=0,\ d_6=0,$$

$$d_7=-\frac{\lambda_1^2-\varepsilon_6}{\varepsilon_7},\ d_8=K\lambda_1\left(\frac{\lambda_1^2-\varepsilon_6}{\varepsilon_7}\right).$$

For incident T-wave:

$$L=L_2,\quad L_1=L_5=L_6=0,$$

$$d_1=-ia,\ d_2=\lambda_2,\ d_3=-\alpha_{12},\ d_4=-\alpha_{22},\ d_5=0,\ d_6=0,$$

$$d_7=-\frac{\lambda_2^2-\varepsilon_6}{\varepsilon_7},\ d_8=K\lambda_2\left(\frac{\lambda_2^2-\varepsilon_6}{\varepsilon_7}\right).$$

For incident SV1-wave:

$$L = L_5, \quad L_1 = L_2 = L_6 = 0,$$

$$d_1 = \lambda_5, \; d_2 = ia, \;\; , \; d_3 = -\beta_{15}, \; d_4 = -\beta_{25}, \; d_5 = -\alpha_{35},$$

$$d_6 = -\frac{\lambda_5^2 - \varepsilon_8}{\varepsilon_9}, \quad d_7 = 0, \quad d_8 = 0.$$

For incident SV2-wave:

$$L = L_6, \quad L_1 = L_2 = L_5 = 0,$$

$$d_1 = \lambda_6, \; d_2 = ia, \quad d_3 = -\beta_{16}, \; d_4 = -\beta_{26}, \; d_5 = -\alpha_{36},$$

$$d_6 = -\frac{\lambda_6^2 - \varepsilon_8}{\varepsilon_9}, \quad d_7 = 0, \quad d_8 = 0.$$

6. Numerical results and discussion

In order to study the wave propagation through an isotropic non-local couple stress micropolar thermoelastic solid, the amplitude ratios corresponding to reflected waves and transmitted waves due to incidence of longitudinal waves (P), thermal waves (T), transverse waves (SV1 and SV2) at free surface have been computed numerically. For the purpose of numerical computations, values of relevant parameters corresponding to two different mediums M and $\bar{M}$ are given in Tab.1.

Table 1. Numerical values of parameters.

Medium M		Medium $\bar{M}$	
Notation	Value	Notation	Value
β_0	$2.68\times10^{10}\ Nm^{-2}$	$\overline{\beta_0}$	$4.0\times10^{12}\ Nm^{-2}$
λ	$18.78\times10^{10}\ Nm^{-2}$	$\bar{\lambda}$	$0.088\times10^{12}\ Nm^{-2}$
μ	$8.76\times10^{10}\ Nm^{-2}$	$\bar{\mu}$	$0.4\times10^{11}\ Nm^{-2}$
α	$17.2\times10^{10}\ N$	$\bar{\alpha}$	$8\times10^{9}\ N$
β	$5.06\times10^{10}\ N$	$\bar{\beta}$	$10^{10}\ N$
Υ	$8.99\times10^{8}\ N$	$\bar{\Upsilon}$	$0.779\times10^{9}\ N$
κ	$8\times10^{10}\ N$	$\bar{\kappa}$	$0.1\times10^{11}\ N$
ρ	174 Kg m^{-3}	$\bar{\rho}$	$233\,Kgm^{-3}$
j	$9.21m^2$	$\bar{j}$	$2.9m^2$
e_0	0.48	$\overline{e_0}$	0.67
a'	$0.543\times10^{-9}\ m$	$\overline{a'}$	$0.421\times10^{-9}\ m$

Cont. Table 1. Numerical values of parameters.

Medium M		Medium $\bar{M}$	
Notation	Value	Notation	Value
C_E	$1.04\times10^3\ Cal K^{-1}$	$\overline{C_E}$	$2.3\times10^3\ Cal K^{-1}$
K	$1.7 J m^{-1}s^{-1}K^{-1}$	$\bar{K}$	$0.016 J m^{-1}s^{-1}K^{-1}$
T_0	$298\ K$	$\overline{T_0}$	$298\ K$
τ_0	$0.8\ s$	$\overline{\tau_0}$	$0.02\ s$

For numerical calculation, other constants are taken as follows:

$$w=2,\ \ \bar{w}=3,\ \ \bar{a}=1.$$

To find amplitude ratios with respect to wave number of the incident longitudinal wave (P), thermal wave (T), and transverse waves (SV1 and SV2), we have used MATLAB software. The amplitude ratios for reflected longitudinal waves, reflected thermal waves, reflected transverse waves in medium M and corresponding transmitted waves in medium $\bar{M}$ are shown graphically. Also, effects of non-local and local parameters on amplitude ratios as a function of wave number of the incident longitudinal wave (P), thermal wave (T), and transverse waves (SV1 and SV2) are compared. For the local parameter, we used $\overline{e_0}=0$. In all graphs, a solid line and a dotted line represent the values of amplitude ratios corresponding to non-local and local parameters, respectively.

6.1. Incident P-wave

The variations of absolute values of the amplitude ratios of various reflected and transmitted waves with respect to the wave number of incident P-wave for $0\le a\le 10$ have been shown in Figs 2-9.
Figure 2 shows the variation of amplitude ratio of reflected P-wave with the wave number of incident P-wave for non-local and local parameter of the micropolar elastic solid. It has been seen that initially the amplitude ratio for the non-local parameter increases and for the local parameter decreases for $0\le a\le 1$. After this, in

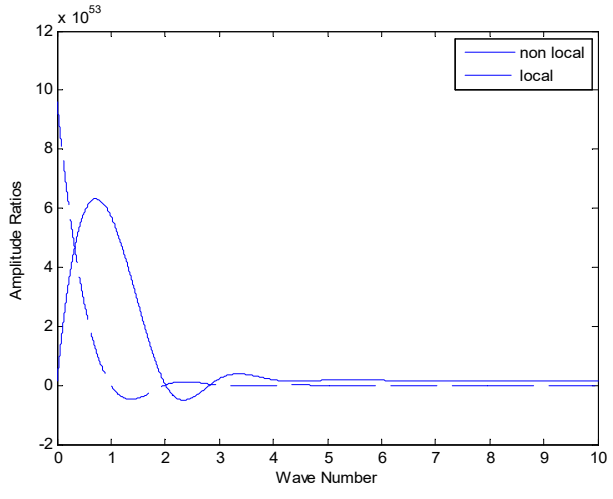

Fig.2. Variations of amplitude ratios of reflected P-wave.

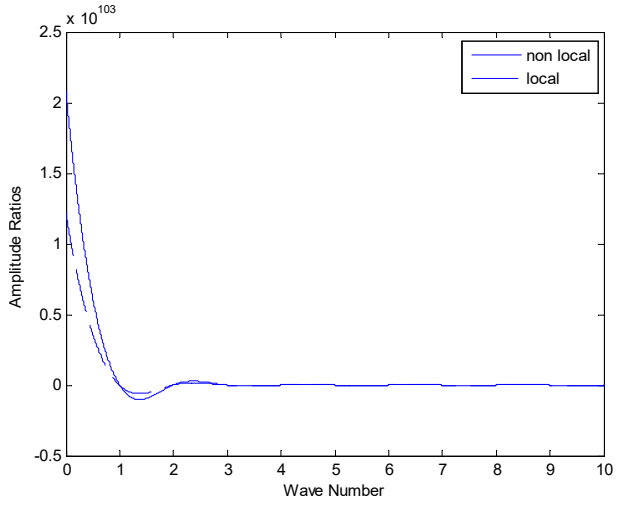

Fig.3.Variations of amplitude ratios of reflected T-wave.

the case of the non-local parameter the amplitude ratio decreases up to $a=2$ and for higher values of wave number, it becomes oscillatory. In the case of the local parameter, the amplitude ratio becomes oscillatory after $a=1$ and onwards. Also, it has been observed that there are some values of wave number corresponding to which the amplitude ratio for the non-local and local parameters coincide. For higher values of wave number, the amplitude ratio for the non-local parameter is higher than the corresponding local elastic solid.

Figure 3 represents variations of amplitude ratio of reflected T-wave with the wave number of incident P-wave for non-local and local parameters of the elastic solid. It is observed that the amplitude ratio has a great decline in its values for $0 \le a \le 1$ in both cases (local as well as non-local). For intermediate and higher values of wave number, the amplitude ratio oscillates.

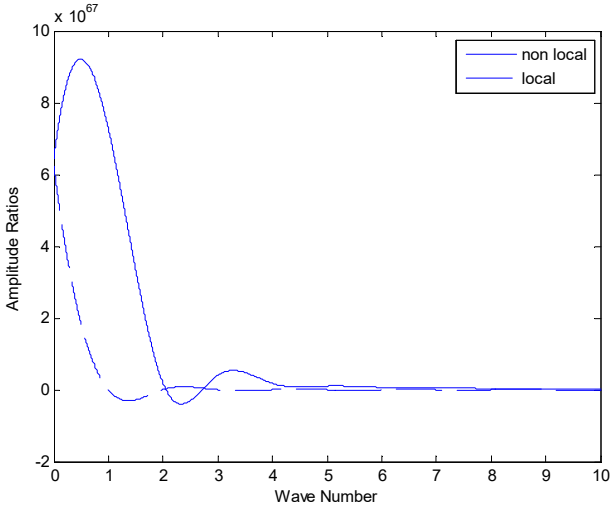

Fig.4.Variations of amplitude ratios of reflected SV1-wave.

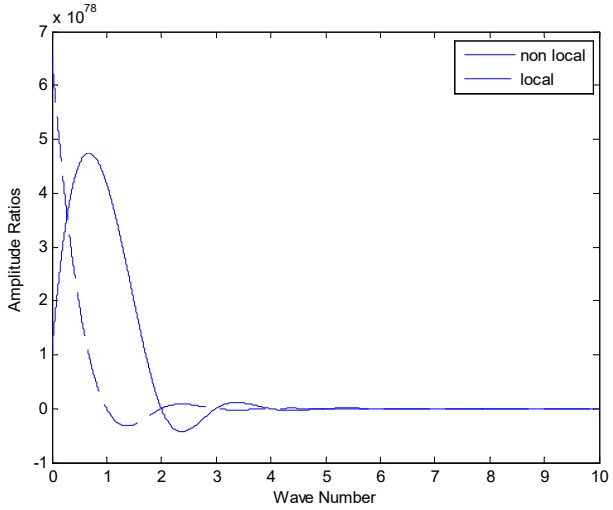

Fig.5. Variations of amplitude ratios of reflected SV2-wave.

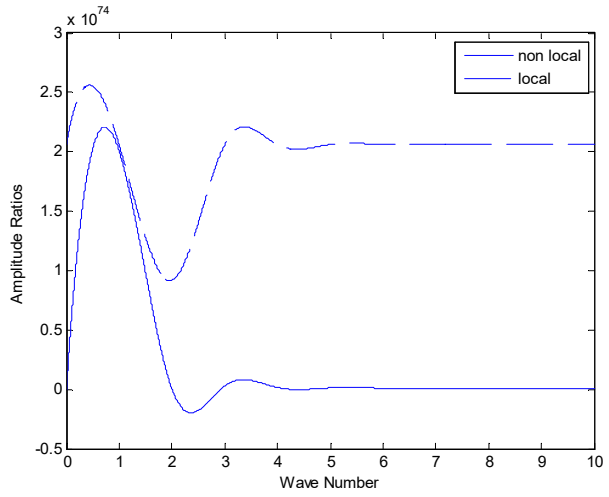

Fig.6. Variations of amplitude ratios of transmitted P-wave.

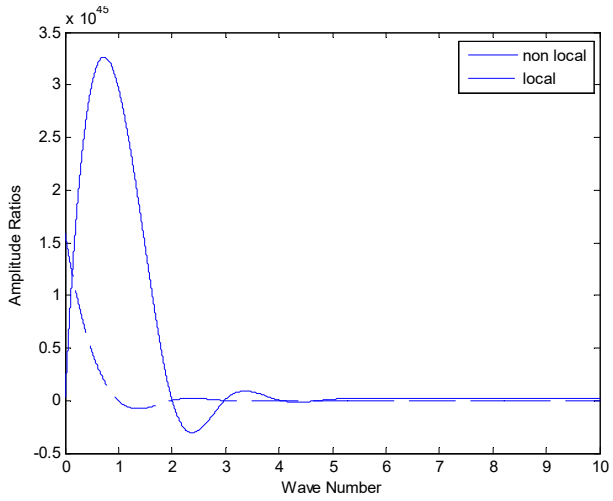

Fig.7. Variations of amplitude ratios of transmitted T-wave.

The variations of amplitude ratio of reflected SV1-wave with the wave number of incident P-wave are shown in Fig.4. For very small values of a, the amplitude ratio $|y_3|$ decreases for the local parameter whereas the

amplitude ratio $|y_3|$ increases for the non-local parameter. For both parameters, the amplitude ratio oscillates corresponding to intermediate and higher values of a and coincides for some values of a.

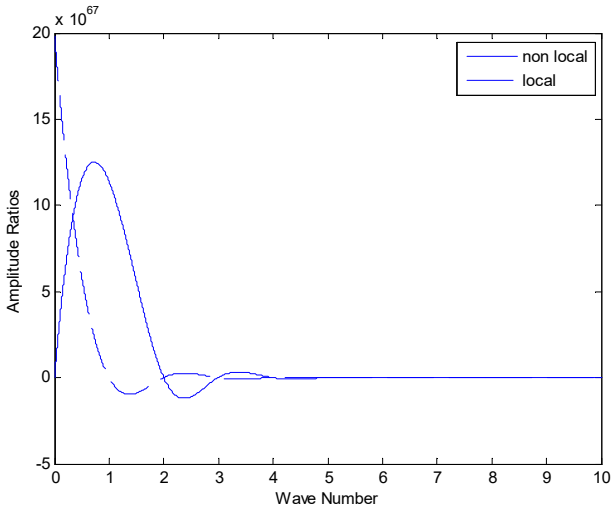

Fig.8. Variations of amplitude ratios of transmitted SV1-wave.

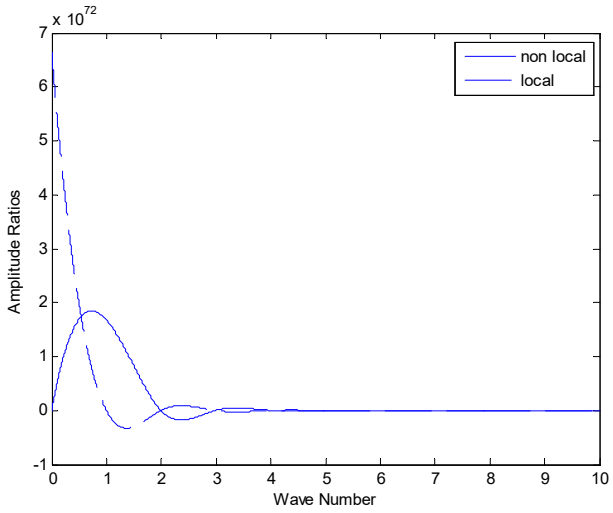

Fig.9. Variations of amplitude ratios of transmitted SV2-wave.

Figure 5 depicts the variations of amplitude ratio of reflected SV2-wave with the wave number of incident P-wave. In $0 \le a \le 1$, there is a point where the amplitude ratio for both parameters are equal. For non-local solid amplitude ratio oscillates for $a \ge 2$ whereas for local solid, it oscillates for $a \ge 2$. For $a \ge 6$ amplitude ratio for both parameters coincide.

It has been observed from Fig.6 that the pattern of variation of amplitude ratio $|y_5|$ (transmitted P-wave) with wave number of incident P-wave is similar for both local and non-local parameters. The value of amplitude ratio firstly increases then decreases for small values of a. For higher values of a, there are small oscillations in both cases. Also, it is observed that the value of $|y_5|$ is greater for the local parameter than for the non-local parameter.

The variations of amplitude ratio of transmitted T-wave with the wave number of incident P-wave are shown in Fig.7. The amplitude ratio for the non-local solid sharply increases in $0 \le a \le 1$ and decreases in $1 \le a \le 2$. For local solid $|y_6|$ sharply decreases in $0 \le a \le 1$, oscillates in $1 \le a \le 5$ and becomes stationary for higher values. Also, there are some values of a for which $|y_6|$ in both cases becomes equal.

From Fig.8, it is clear that the behavior of amplitude ratio $|y_7|$ for transmitted SV1-wave is similar to $|y_6|$ in $0 \le a \le 1$ with a difference in the magnitude values. For $5 \le a \le 10$ the amplitude ratio $|y_7|$ for both local and non-local solid coincides.

Figure 9 shows the variations of amplitude ratio $|y_8|$ for transmitted SV2-wave. For $0 \le a \le 1$, there is a sharp decrease in the amplitude ratio for local solid, whereas the value of amplitude ratio increases gradually for non-local solid. For higher values of the wave number the amplitude ratio for both type of solids coincides.

6.2. Incident T-wave

Figure 10 shows that behavior of the amplitude ratio $|y_1|$ for reflected P-wave (for incident T-wave) is similar to $|y_8|$ for transmitted SV2-wave (for incident of P-wave) in $0 \le a \le 1$ with difference in the

magnitude values. For $a \geq 4$, the amplitude ratio for the non-local solid increases sharply whereas decreases very slowly for the local solid. Also, magnitude for the non-local solid is much higher than for the local solid corresponding to higher values of wave number.

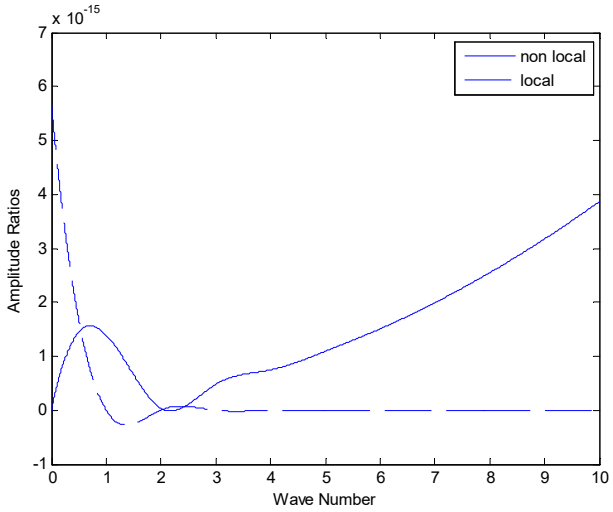

Fig.10. Variations of amplitude ratios of reflected P-wave.

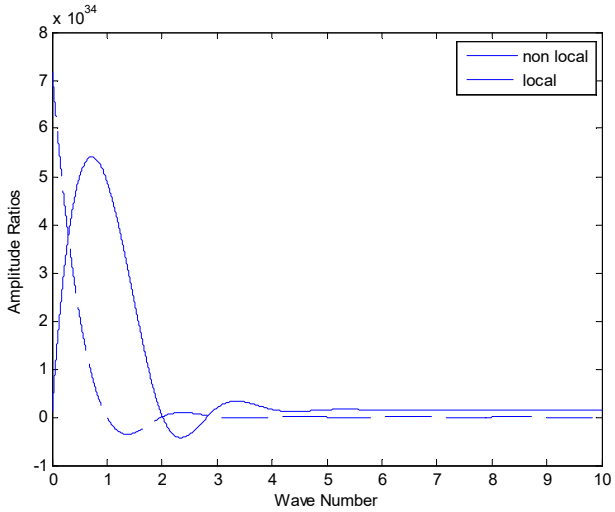

Fig.11. Variations of amplitude ratios of reflected T-wave.

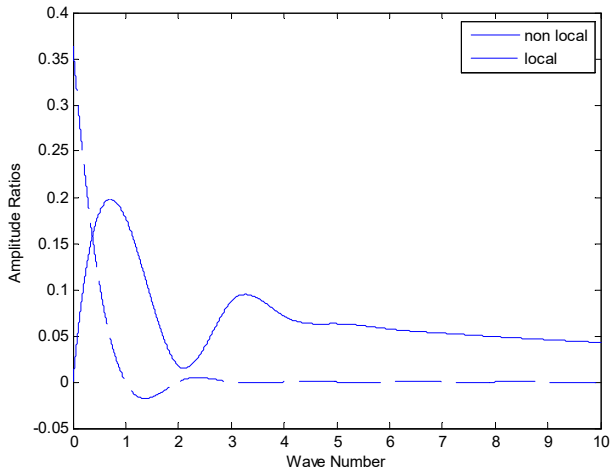

Fig.12.Variations of amplitude ratios of reflected SV1-wave.

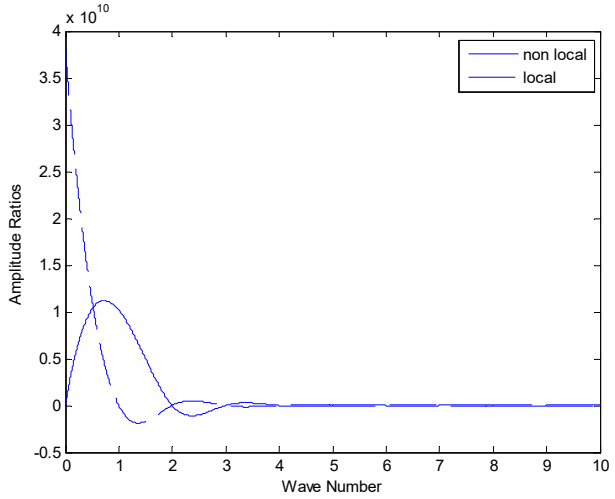

Fig.13. Variations of amplitude ratios of reflected SV2-wave.

It has been observed from Fig. 11 that the behavior of the amplitude ratio $|y_2|$ for reflected T-wave (for incident T-wave) is similar to $|y_7|$ for transmitted SV-1 wave (for incident P-wave) in $0 \leq a \leq 2$ with difference in the magnitude values. There are three points where amplitude ratios for both (local and non-local) type of solids coincide. For $a \geq 3$ value of amplitude ratio for the non-local solid is greater than that of the local solid.

Figure 12 depicts the variation of the amplitude ratio $|y_3|$ for reflected SV-1-wave with the wave number of incident T-wave. It has been observed that there is only one point where the graph of both solid crosses. Initially, the amplitude ratio for local elastic solids decreases sharply whereas for the non-local solid,

the amplitude ratio increases. For $1 \le a \le 4$, the amplitude ratio oscillates in both graphs with different magnitude and for higher values of a, the value of the amplitude ratio decreases continuously.

From Fig.13 it is clear that the behavior of the amplitude ratio $|y_4|$ for reflected SV-2 wave (for incident T-wave) is similar to $|y_8|$ for transmitted SV-2 wave (for incident P-wave) in $0 \le a \le 4$ with difference in the magnitude values. For a higher value of wave number, the amplitude ratio for the local and non-local solid is approximately same.

Figure 14 shows the variation of the amplitude ratios $|y_5|$ for transmitted P-wave. For the non-local solid the amplitude ratio increases sharply for $0 \le a \le 1$ and decreases sharply for $1 \le a \le 2$. For $2 \le a \le 4$, it oscillates and increases continuously for higher values of a. For the local solid, the amplitude ratio increases smoothly for $a \ge 2$ and for $a \le 2$, it fluctuates slowly.

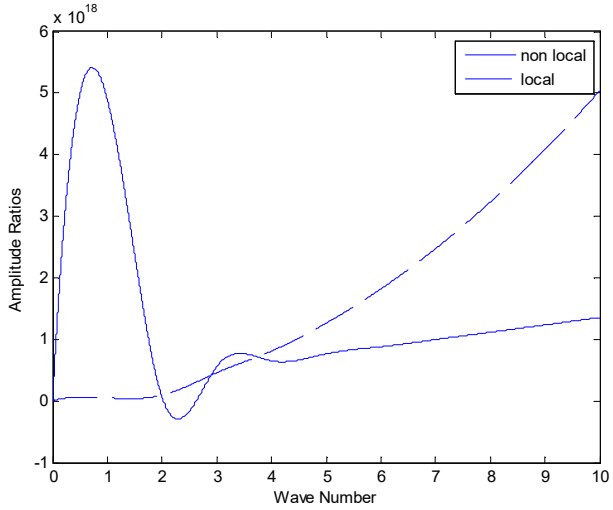

Fig.14. Variations of amplitude ratios of transmitted P-wave.

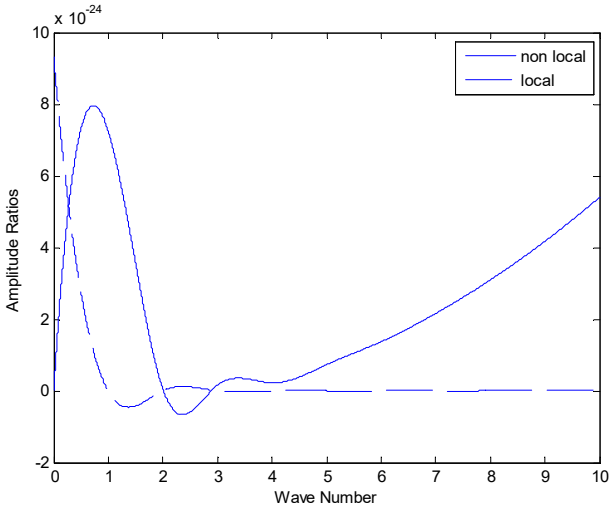

Fig.15. Variations of amplitude ratios of transmitted T-wave.

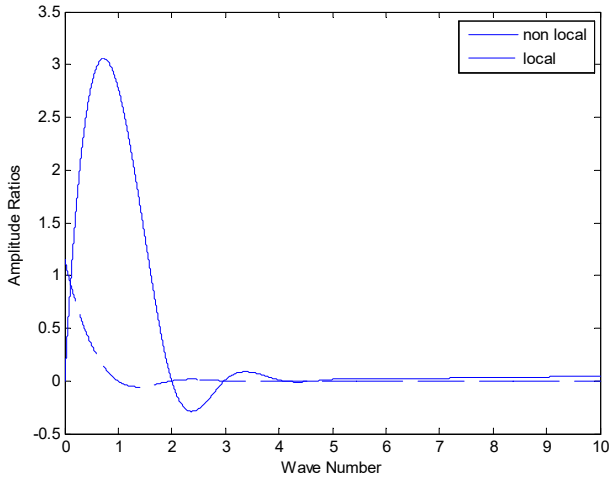

Fig.16. Variations of amplitude ratios of transmitted SV1-wave.

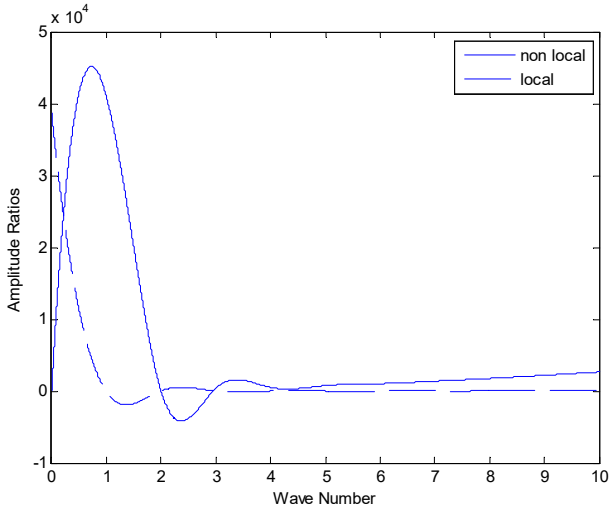

Fig.17. Variations of amplitude ratios of transmitted SV2-wave.

Figure 15 shows that for the local solid, variation of the amplitude ratio $|y_6|$ for transmitted T-wave (for incident T-wave) is similar to the variation of the amplitude ratio of reflected SV2-wave (for incident P-wave) with difference in magnitude. For the non-local solid, for $0 \le a \le 4$, the variation of the amplitude ratio is same as the variation of the amplitude ratio $|y_5|$ for transmitted P-wave (when T-wave is incident) with difference in magnitude.

For higher values of a, the amplitude ratio for non-local solid is much higher than that of the local solid. The variations of the amplitude ratio $|y_7|$ of transmitted SV1-wave with the wave number of incident T-wave is shown in Fig.16. For the non-local solid, the behavior of the amplitude ratio is similar to the behavior of the amplitude ratio $|y_2|$ for reflected T-wave (for incident T-wave) with difference in magnitude. For the local solid the amplitude ratio decreases initially for $0 \le a \le 1$ and remains constant for higher values of a.

From Fig.17, it is clear that the behavior of the amplitude ratio $|y_8|$ for transmitted SV2-wave is similar to the behavior of the amplitude ratio $|y_2|$ for reflected T-wave (for incident T-wave) with difference in magnitude.

6.3. Incident SV1-wave

It is clear from the Fig.18 that the behavior of the amplitude ratio $|y_1|$ for reflected P-wave with respect to wave number of incident SV1-wave is similar to the behavior of the amplitude ratio $|y_2|$ for reflected T-wave with respect to the wave number of incident T-wave with difference in magnitude.

From Fig.19 it is observed that variations of the amplitude ratio $|y_2|$ with respect to the wave number of incident SV1-wave is similar in both (local and non-local) type of solid with difference in magnitude values. For $0 \le a \le 1$ the amplitude ratio increases sharply and then decreases for $1 \le a \le 2$. For $a \ge 2$ variation is very small.

Variations of the amplitude ratio for reflected SV1-wave with the wave number of incident SV1-wave are shown in Fig.20. It is clear that the amplitude ratio $|y_3|$ increases with an increase in the wave number of incident wave in both type of solid (local and non-local). The Magnitude of the amplitude ratio for the non-local solid is more than that of the local solid corresponding to same wave number.

Figure 21 shows that the amplitude ratio for reflected SV2-wave decreases smoothly in $0 \le a \le 1$ for the local solid whereas for the non-local solid it decreases in $0 \le a \le 2$. For $a \ge 1$, for the local solid and for $a \ge 2$, for the non-local solid, the variations in the amplitude ratio are very small with respect to the wave number.

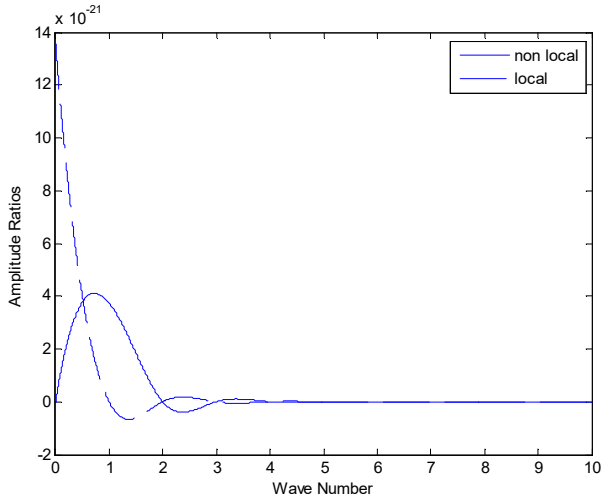

Fig.18. Variations of amplitude ratios of reflected P-wave.

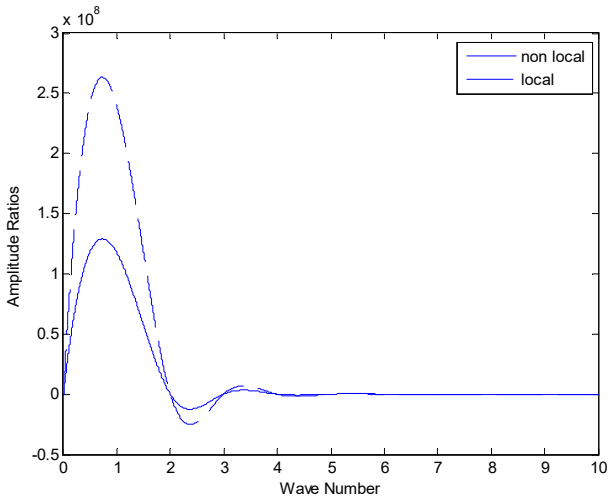

Fig.19. Variations of amplitude ratios of reflected T-wave.

Figure 22 shows the behavior of transmitted P-wave when SV1-wave is incident. For the local solid, the amplitude ratio decreases initially for very small values of $'a'$ and then increases up to a maximum value corresponding to $a=2$. After $a=2$ variations are very small. In the non-local solid, for $0\le a\le 1$ the amplitude ratio increases sharply and then decreases for $1\le a\le 2$. For $a\ge 2$ variations are very small.

It is observed from Fig.23 that the behavior of the amplitude ratio $|y_6|$ for transmitted T-wave with respect to the wave number of incident SV1-wave is similar to the behavior of the amplitude ratio $|y_7|$ for transmitted SV1-wave with respect to the wave number of incident P-wave with difference in magnitude values.

It is clear from Figs 24 and 25 that the behavior of the amplitude ratio $|y_7|$ for transmitted SV1-wave and $|y_8|$ for transmitted SV2-wave with respect to the wave number of incident SV1-wave is similar to the behavior of the amplitude ratio $|y_2|$ for reflected T-wave with respect to the wave number of incident SV1-wave with difference in magnitude values.

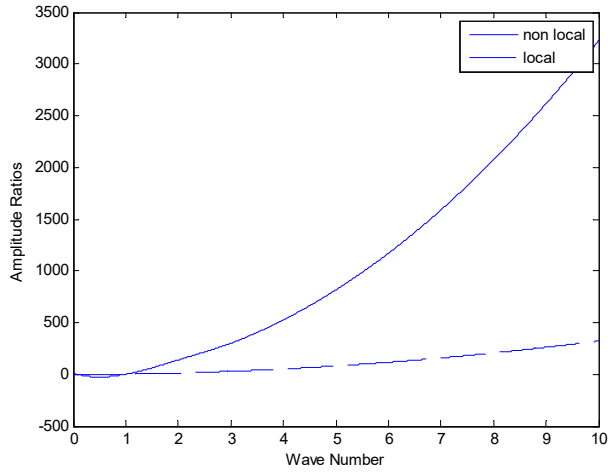

Fig.20. Variations of amplitude ratios of reflected SV1-wave.

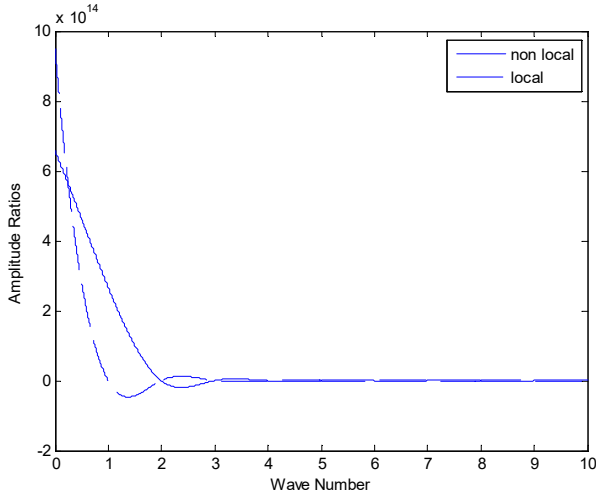

Fig.21. Variations of amplitude ratios of reflected SV2-wave.

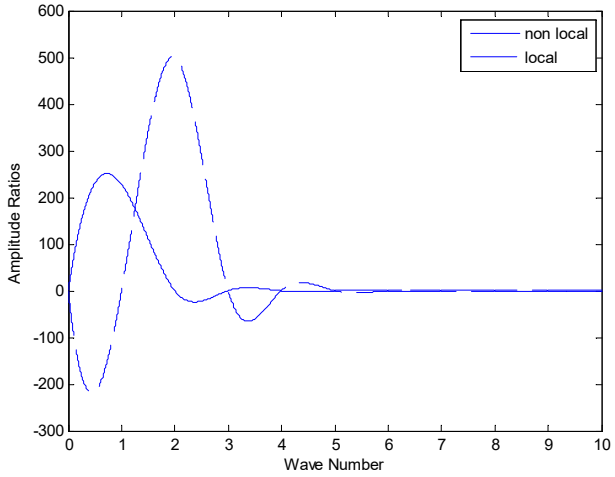

Fig.22. Variations of amplitude ratios of transmitted P-wave.

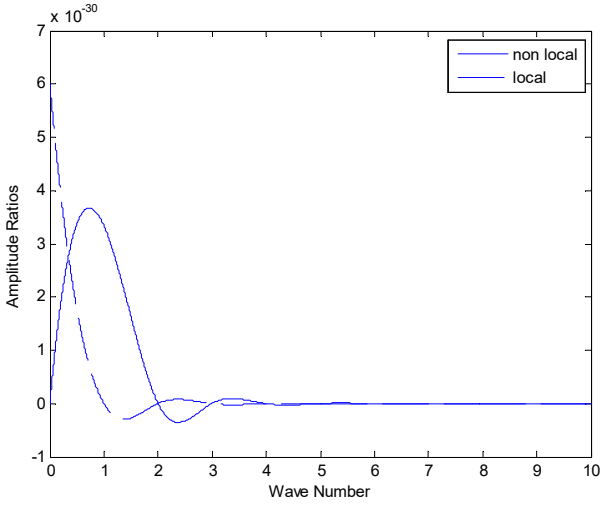

Fig.23. Variations of amplitude ratios of transmitted T-wave.

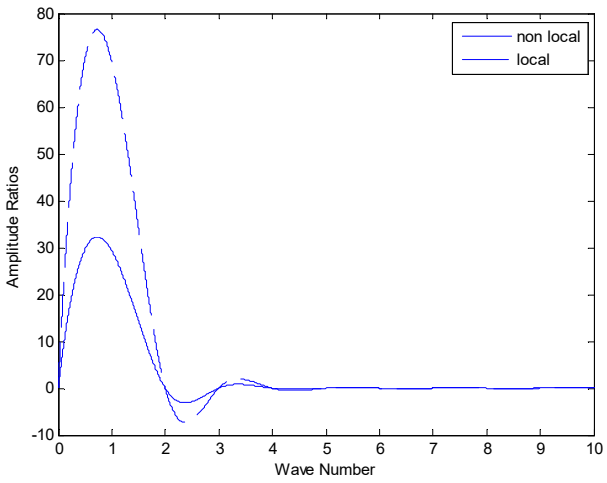

Fig.24. Variations of amplitude ratios of transmitted SV1-wave.

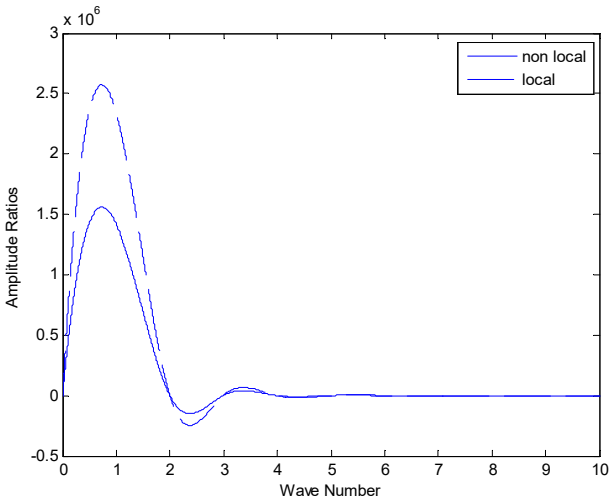

Fig.25. Variations of amplitude ratios of transmitted SV2-wave.

6.4. Incident SV2-wave

Figure 26 shows the variations of the amplitude ratio of reflected P-wave with respect to the wave number of incident SV2-wave for the non-local and local micropolar elastic solid. In the local solid the amplitude ratio decreases for $0 \le a \le 1$. For $a \ge 1$ the amplitude ratio becomes oscillatory. For the non-local solid, for $0 \le a \le 5$ the amplitude ratio is constant and for $a \ge 5$ it becomes oscillatory. Also, there are some values of 'a' corresponding to which the amplitude ratio coincides for both types of solid.

It is clear from Fig.27 that there is only one value of 'a' corresponding to which the amplitude ratio for both solids (local and non-local) coincides. For $a \le 2$, the amplitude ratio of the non-local solid is more than that of the local solid while for $a \ge 2$ the amplitude ratio of the local solid is more than that of the non-local solid.

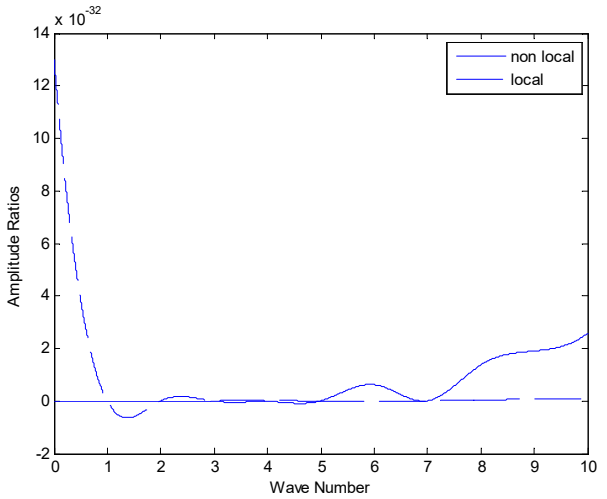

Fig.26. Variations of amplitude ratios of reflected P-wave.

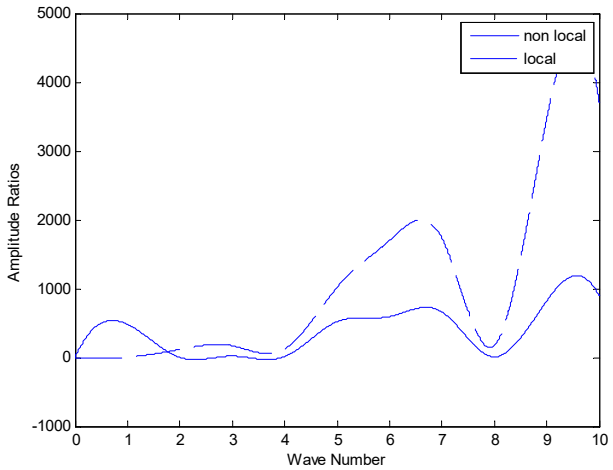

Fig.27.Variations of amplitude ratios of reflected T-wave.

Variations of the amplitude ratio for reflected SV1-wave with the wave number of incident SV2-wave are shown in Fig.28. It is clear that the amplitude ratio $|y_3|$ increases with an increase in the wave number of

incident wave in both type of solid (local and non-local). The Magnitude of the amplitude ratio for the local solid is more than that of the non-local solid corresponding to same wave number.

It is clear from Fig.29 that the behavior of the amplitude ratio $|y_4|$ for reflected SV2-wave with respect to the wave number of incident SV2-wave is similar to the behavior of the amplitude ratio $|y_3|$ for reflected SV1-wave with respect to the wave number of incident SV1-wave with difference in magnitude values.

Figure 30 shows that the behavior of transmitted P-wave for the local solid (when SV2-wave is incident) is similar to the behavior of transmitted P-wave (when SV1-wave is incident). For the non-local solid, the amplitude ratio oscillates for $0 \le a \le 4$ and for $a \ge 4$, it increases smoothly.

It has been observed from Fig.31 that the behavior of the amplitude ratio $|y_6|$ for transmitted T-wave with respect to the wave number of incident SV2-wave is similar to the behavior of the amplitude ratio $|y_1|$ for reflected P-wave with respect to the wave number of incident T-wave with difference in magnitude values.

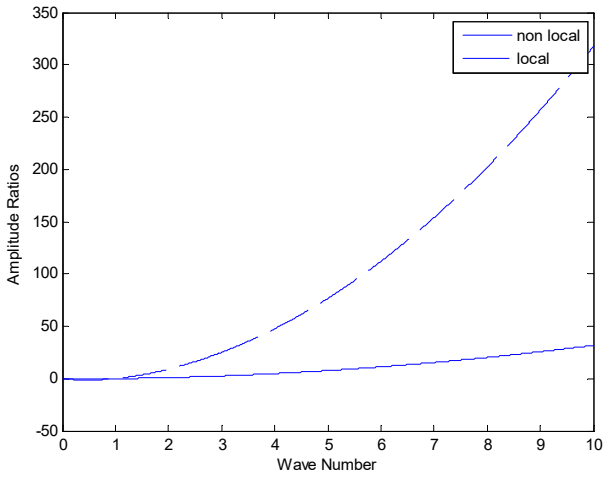

Fig.28. Variations of amplitude ratios of reflected SV1-wave.

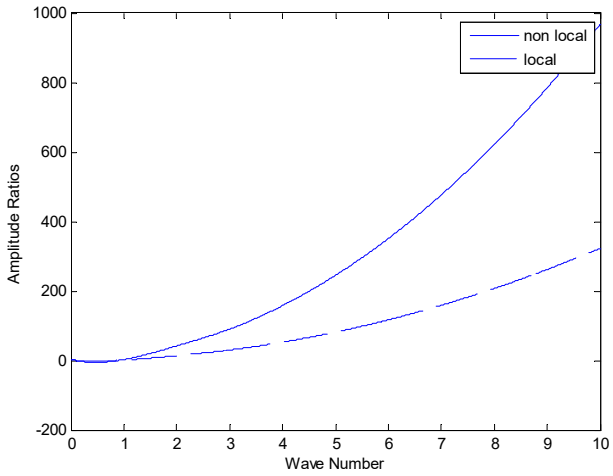

Fig.29. Variations of amplitude ratios of reflected SV2-wave.

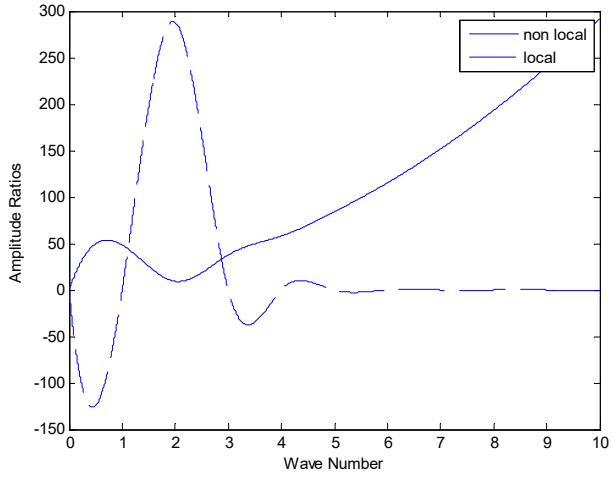

Fig.30. Variations of amplitude ratios of transmitted P-wave.

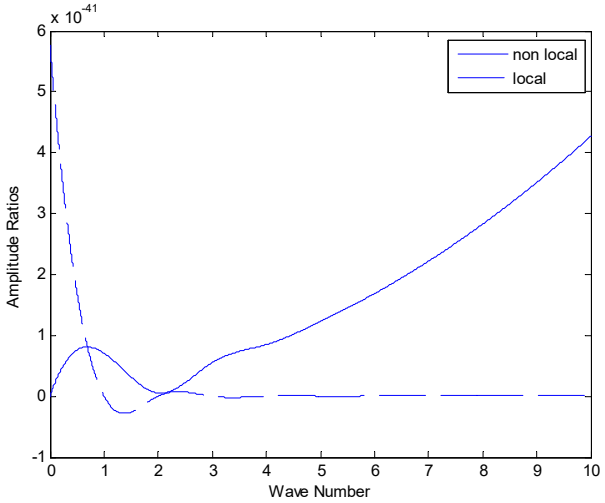

Fig.31. Variations of amplitude ratios of transmitted T-wave.

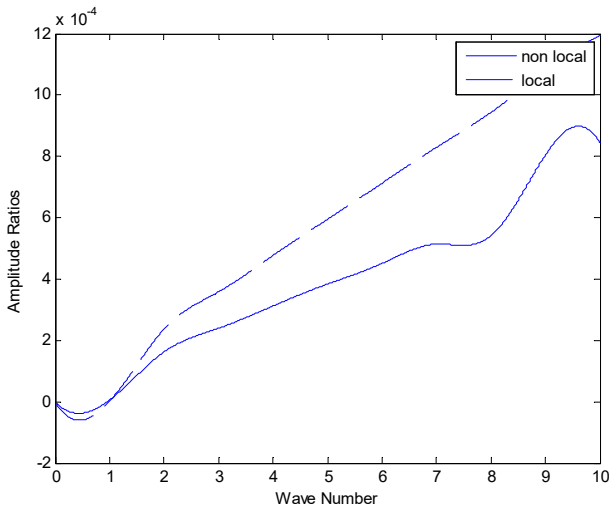

Fig.32. Variations of amplitude ratios of transmitted SV1-wave.

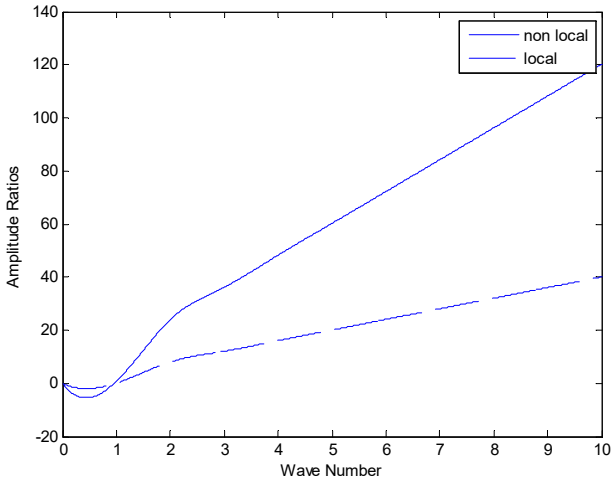

Fig.33. Variations of amplitude ratios of transmitted SV2-wave.

From Figs 32 and 33 it is clear that the amplitude ratio $|y_7|$ for transmitted SV1-wave and $|y_8|$ for transmitted SV2-wave increases with an increase in the wave number of incident SV2-wave except some points. In both graphs, there is only one point where amplitude ratios for the local and non-local solid coincides. For $a \geq 1$, for transmitted SV1-wave the amplitude ratio for the local solid is more than that of the non-local solid while for transmitted SV2-wave the amplitude ratio for the non-local solid is more than that of the local solid.

7. Conclusions

In the present work, we have obtained the expressions for the amplitude ratios of reflection and transmission of waves at the interface of two distinct homogenous, isotropic non-local couple stress micropolar thermoelastic solids. The variations in absolute values of the amplitude ratios of various reflected and transmitted waves with respect to wave number of incident P-, T-, SV1-, SV2-waves are shown graphically in the local as well as the non-local solid. It is observed that the non-local parameter plays a vital role in reflection and transmission phenomenon. Results obtained from the graphs of this model may be very useful for scientists working in various fields of mechanics.

Nomenclature

a' – characteristic length
C_E – specific heat
e_{ijk} – permutation symbol
e_0 – material constant
j – micro-inertia
K – thermal conductivity
T – temperature change measured from the absolute temperature T_0
$\boldsymbol{u}$ – displacement vector
Y – $= (3\lambda + 2\mu)\beta_0$
$\alpha, \beta, \Upsilon, \kappa$ – micropolar constants
β_0 – coefficient of linear thermal expansion
δ_{ij} – Kronecker delta
$\varepsilon = e_0 a'$ – non-local parameter

λ and μ – Lame's constants
μ_{ij} – components of couple stress
ρ – density of medium
σ_{ij} – stress components
τ_0 – relaxation time
$\boldsymbol{\varphi}(0,\varphi,0)$ – rotational vector
∇^2 – Laplacian operator

REFERENCES

[1] Eringen A.C. (1966): *Linear theory of micropolar elasticity.*– Mathematics and Mechanics, vol.15, No.6, pp.909-923.

[2] Eringen A.C. (1972): *Linear theory of non-local elasticity and dispersion of plane waves.*– Int. J. Eng Sci., vol.10, pp.425-435.

[3] Eringen A.C. and Edelen D.G.B. (1972): *On nonlocal elasticity.*– Int. J. Eng. Sci., vol.10, No.3, pp.233-248.

[4] Chandrasekharaiah D.S. (1983): *Surface waves in micropolar thermoelasticity*.– Proc. Indian Acad. Sci.(Math. Sci.), vol.92, No.6, pp.109-120.

[5] Eringen A.C. (1990): *Theory of thermo-microstretch elastic solids*.– Int. J. Engng. Sci., vol.28, No.12, pp.1291-1301.

[6] Inan E. and Eringen A.C.(1991): *Nonlocal theory of wave propagation in thermoelastic plates.*– Int. J. Engng. Sci., vol.29, No.7, pp.831-843.

[7] Eringen A.C. (2002): *Non-Local Continuum Field Theories*.– New York, Springer-Verlag.

[8] Kumar R. and Deswal S. (2002): *Surface wave propagation in a micropolar thermoelastic medium without energy dissipation.*– Journal of Sound and Vibrations, vol.256, pp.173-178.

[9] Kumar R. and Chawla V. (2012): *Reflection and transmission of plane waves at an interface between elastic and micropolar diffusion media.*– Canadian Applied Mathematics Quarterly, vol.20, pp.375.

[10] Kumar R. and Gupta V. (2013): *Reflection and transmission of plane waves at the interface of an elastic half-space and a fraction order thermoelastic half-space.*– Archieve of Applied Mechanics, vol.83, pp.1109-1128.

[11] Kumar M., Kaur M. and Rajvanshi S.C. (2014): *Reflection and transmission between two micropolar thermoelastic half-spaces with three-phase-lag model.*– Journal of Engineering Physics and Thermodynamics, vol.87, No.2, pp.295-307.

[12] Kumar R. (2015): *Wave propagation in microstretch thermoelastic diffusion solid*.– An. St. Univ. Ovidius Constanta, vol.23, No.1, pp.127-169.

[13] Kumar R,. Kumar K. and Nautiyal R.C. (2015): *Reflection at the free surface of couple stress generalised thermoelastic solid half space*.– Open Journal of Heat, Mass and Momentum Transfer, vol.3, No.1, pp.14-28.

[14] Khurana A. and Tomar S.K. (2016): *Wave propagation in nonlocal microstretch solid*.– Applied Mathematical Modelling, vol.40, pp.5858-5875.

[15] Kumar R. and Kumar K. (2016): *Reflection and transmission at the boundary surface of modified couple stress thermoelastic media*.– Int. J. of Applied Mechanics and Engineering, vol.21, No.1, pp.61-81.

[16] Khurana A. and Tomar S.K. (2017): *Rayleigh-type waves in nonlocal micropolar solid half-space.*– Ultrasonics, vol.73, pp.162-168.

[17] Singh D., Kaur G. and Tomar S.K. (2017): *Waves in nonlocal elastic solid with voids*.– Journal of Elasticity, vol.128, pp.85-114.

[18] Khurana A. and Tomar S.K. (2018): *Waves at interface of dissimilar nonlocal micropolar elastic half-spaces*.– Mechanics of Advanced Materials and Structures, vol.26, No.3, pp.1-9.

[19] Kaur G., Singh D. and Tomar S.K. (2018): *Rayleigh-type wave in a nonlocal elastic solid with voids*.– European Journal of Mechanics / A Solids, vol.71, pp.134-150.

[20] Kaur G., Singh D. and Tomar S.K. (2019): *Love waves in a nonlocal elastic media with voids.*– Journal of Vibration and Control, vol.25, No.8, pp.1-14.

[21] Sarkar N. and Tomar S.K. (2019): *Plane waves in nonlocal thermoelastic solid with voids.*– Journal of Thermal Stress, vol.42, No.5, pp.1-27.

[22] Sarkar N., De S., and Sarkar N. (2019): *Waves in nonlocal thermoelastic solids of type II.*– Journal of Thermal Stress, vol.42, No.9, pp.1153-1170.

[23] Singh B., Yadav A.K. and Gupta D. (2019): *Reflection of plane waves from a micropolar thermoelastic solid half-space with impedance boundary conditions*.– Journal of Ocean Engineering and Science, vol.4, pp.122-131.

[24] Das N., De S. and Sarkar N. (2020): *Reflection of plane waves in generalised thermoelasticity of type III with nonlocal effect*.– Mathematical Methods in the Applied Sciences, vol.43, No.3, pp.1313-1336.

[25] Biswas S. (2020): *Rayleigh waves in a nonlocal thermoelastic layer lying over a nonlocal thermoelastic half space.*– Acta Mechanica, vol.231, pp.4129-4144.

[26] Sarkar N., Abo-Dohab S.M. and Mondal S. (2020): *Reflection of magneto-thermoelastic waves at a solid half-space under modified Green-Lindsay model with two temperatures.*– Journal of Thermal Stress, vol.43, No.9, pp.1083-1099.

[27] Pramanik A.S. and Biswas S. (2020): *Surface waves in non-local thermoelastic medium with state space approach.*– Journal of Thermal Stress, vol.43, No.6, pp.1-20.

[28] Poonam, Sahrawat R.K. and Kumar K. (2021): *Plane wave propagation and fundamental solution in non-local couple stress micropolar thermoelastic solid medium with voids.*– Waves in Random and Complex Media, vol.31, pp.1-37.

[29] Kaur I. and Singh K. (2021): *Plane wave in non-local semiconducting rotating media with Hall effect and three phase lag fractional order heat transfer*.– International Journal of Mechanical and Materials Engineering, vol.14, pp.1-16.

Received: November 11, 2021
Revised: March 1, 2022